Eurasian Chem.-Technol. J. 27 (2025) 269–279
The journal of the Institute of Combustion Problems https://ect-journal.kz

https://doi.org/10.18321/ectj1674

Molecular Modelling of Cyclodextrin Inclusion Complexes of 2-((Morpholinoimino)Methyl)Benzoic Acid and its Heterocyclic Derivative

O.A. Nurkenov[1,2], S.D. Fazylov[1]*, A.K. Syzdykov[1,2], Z.M. Muldakhmetov[1], A.R. Kovrizhina[3], A.I. Khlebnikov[3,4], T.M. Seilkhanov[5], S.K. Kabiyeva[2], A.T. Takibayeva[6], A.Zh. Mendibayeva[1,2]

[1]Institute of Organic Synthesis and Coal Chemistry of the Republic of Kazakhstan, 1 Alikhanov St., Karaganda, Kazakhstan
[2]Karaganda Industrial University, 30 Republic Ave., Temirtau, Kazakhstan
[3]N.M. Kizhner Research Center, Tomsk Polytechnic University, 30 Lenin Ave.,Tomsk, Russia
[4]National Research Tomsk State University, 36 Lenin Ave., Tomsk, Russia
[5]Sh. Ualikhanov Kokshetau University, 76 Abay St., Kokshetau, Kazakhstan
[6]Abylkas Saginov Karaganda Technical University, 56 Nursultan Nazarbayev Ave.,Karaganda, Kazakhstan

Article info

Received:
10 July 2025

Received in revised form:
25 August 2025

Accepted:
16 October 2025

Keywords:
N-aminomorpholine hydrazone
Phthalimidine
β-cyclodextrin
Complexation
^{1}H and ^{13}C NMR spectra
Molecular modelling

Abstract

This study investigates the formation and characteristics of inclusion complexes between β-cyclodextrin and two compounds: N-aminomorpholine hydrazone and its phthalimidine derivative. Structural features of the encapsulated forms of these new N-aminomorpholine derivatives were characterized using ^{1}H and ^{13}C NMR spectroscopy, as well as two-dimensional ^{1}H–^{1}H (COSY) and ^{1}H–^{13}C (HMBC, HSQC) NMR experiments. Using molecular modeling methods, the influence of structural factors and the principle of geometric complementarity on the complexation processes between the host and guest molecules were assessed. A conformational study of the guest molecules was carried out using the semiempirical GFN2-xTB method in combination with the GOAT algorithm. Employing density functional theory (DFT), the inclusion complexes were optimized at the ωB97X-D/6-311G(d,p) level, including aqueous solvation effects as described by the CPCM model. The thermodynamic parameters of complex formation were estimated. NMR analysis confirmed 1:1 stoichiometry and showed significant chemical shift perturbations for cavity protons, while DFT calculations revealed spontaneous complexation (ΔG°_{298} = −2.54 to −3.45 kcal/mol) driven by exothermic enthalpies and hydrophobic/van der Waals interactions, with an enantioselective preference for the *R*-phthalimidine enantiomer. These findings demonstrate β-CD's potential to enhance the solubility, stability, and bioavailability of these promising antiviral and antibacterial agents for pharmaceutical applications.

1. Introduction

The use of heterocyclic compounds as starting materials in drug discovery is an important strategy in medicinal chemistry. Heterocyclic compounds are versatile building blocks that can be modified to create various chemical structures with a wide variety of biological activities. By making minor changes to the structure of a heterocyclic compound, researchers can fine-tune its properties to optimize pharmacological effects. Heterocycles are widely distributed in nature and are found in many biologically active molecules, making them an attractive starting point for drug discovery. By studying the chemical composition of these compounds, researchers can identify new drug candidates with improved activity, selectivity, and safety. Overall, the use of heterocyclic compounds in drug discovery offers a promising approach to developing new pharmacologically relevant agents that can effectively treat various diseases [1–3].

*Corresponding author.
E-mail address: faz8990@mail.ru

In recent years, a number of review publications have appeared describing the use of natural and synthetic macrocyclic compounds (crown ethers, cryptands, oligosaccharides, etc.) in the development of new-generation drugs [4–6]. Among them, complexes of natural cyclic oligosaccharides (cyclodextrins, CDs) with biologically active molecules, due to the interest of pharmaceutical companies, are one of the most intensively studied objects in the chemistry of inclusion compounds. Encapsulation of a medicinal substrate, i.e. placing it in an internal protective shell of macrocycles, is one of the ways to improve the quality of biologically active drugs by reducing the impact of external factors and ensuring their prolonged action. This leads to the preservation of the physicochemical properties of the "guest molecule", such as stability, bioavailability, and increases their solubility in aqueous and physiological environments. Various water-soluble polysaccharides are capable of forming complexes with a wide range of pharmaceutical molecules, providing modifications of the quality characteristics of molecules with medicinal action. The main results of these studies are the discovered effects of increasing the solubility of organic compounds in the composition of complexes with CDs, increasing their stability in the environment of physiological fluids and during storage, improving taste qualities, enhancing pharmacological activity, prolonging the therapeutic effect, reducing side effects, etc. Under these conditions, known medicinal substances in inclusion complexes with molecules of CD macrocycles or their derivatives acquire new useful characteristics that are not characteristic of the original substrates, which enhances their therapeutic effect. The present study extends our prior investigations into the synthesis of inclusion complexes [7] and hydrazide-hydrazone derivatives [8], focusing on novel analogs with anticipated biological properties.

2. Results and Discussions

Previously [9] during studies of the antiviral activity of N-aminomorpholine hydrazones, a pronounced virus-inhibiting effect of 2-((morpholinoimino) methyl)benzoic acid (**2**) was established against influenza virus strains with different antigenic formulas: A/Almaty/8/98 (H3N2) and A/Vladivostok/2/09 (H1N1). Compound **2** demonstrated a high chemotherapeutic index and exhibited antiviral activity comparable to that of commercially available anti-influenza drugs, positioning it as a promising candidate for the development of novel influenza therapeutics. Notably, morpholine derivative **2** has pronounced antibacterial activity against the Gram-negative strain *Escherichia coli* ATCC 25922, with a minimum inhibitory concentration (MIC) of 6.3 μg/mL. It also demonstrated moderate antimicrobial activity against the Gram-positive strain *Staphylococcus aureus* ATCC 6538.

Hydrazone **2** was prepared by condensing N-aminomorpholine (**1**) with 2-formylbenzoic acid. Treatment of **2** with acetic anhydride then yielded the novel phthalimidine derivative **3** [9] (Scheme 1).

In order to obtain new oligosaccharide inclusion complexes, we used hydrazone **2** and phthalimidine **3** as guest molecules. The inclusion complexes of β-CD with 2-((morpholinoimino)methyl)benzoic acid **2**⊂β-CD and 2-morpholino-3-oxo-isoindolin-1-yl acetate **3**⊂β-CD were obtained by heating equimolar mixtures (1:1) of the host and guest in ethyl alcohol at 50–70 °C for 3–4 hours.

Analysis of the structural features of the obtained inclusion complexes **2**⊂β-CD and **3**⊂β-CD was carried out using the NMR method on ^{1}H and ^{13}C nuclei [10]. NMR analysis reveals significant chemical shift perturbations for protons H-3 and H-5 of β-CD – located within the hydrophobic cavity – upon inclu-

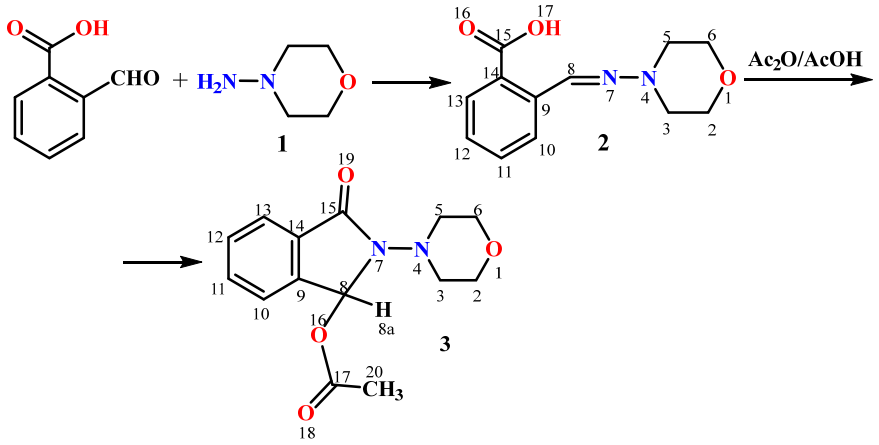

Scheme 1. Synthesis of the hydrazone and phthalimidine derivatives.

sion of the guest molecule. In contrast, peripheral protons H-1, H-2, and H-4 usually show negligible shifts, consistent with their solvent-exposed positions [11–13].

The ^{1}H NMR spectrum of the inclusion complex **2**⊂β-CD in DMSO-d_6 is characterized by the presence of two four-proton doublets assigned to the morpholine fragment H-3,3,5,5 and H-2,2,6,6 (Scheme 1) at 3.05 and 3.72 ppm, respectively, with 3J 3.4 Hz (Table 1). Aromatic protons appeared as single-proton multiplets at 7.29-7.34 (H-11), 7.44-7.49 (H-12), 7.77-7.80 (H-10) and 7.85-7.88 (H-13) ppm. Azomethine proton H-8 was registered as single-proton multiplet at 8.31–8.32 ppm. Carboxyl proton H-17 did not appear in the spectrum due to the proton-deuterium exchange or salt formation. In the ^{13}C NMR spectrum (DMSO-d_6) of the **2**⊂β-CD inclusion complex, signals of morpholine carbon atoms appeared at 51.93 (C-3,5) and 66.16 (C-2,6) ppm. Aromatic carbon atoms are observed at 126.22 (C-13), 128.10 (C-11), 130.78 (C-10), 132.13 (C-12,14), and 134.70 (C-9) ppm. The azomethine carbon atom C-8 resonated at 136.72 ppm. In the downfield region, a signal of the carboxyl atom C-15 was observed at 168.99 ppm.

The structure of the **2**⊂β-CD inclusion complex was also confirmed by two-dimensional COSY (^{1}H–^{1}H) and HMQC (^{1}H–^{13}C) NMR spectroscopy methods, which made it possible to establish spin-spin interactions of homo- and heteronuclear nature. Some of the observed correlations in the molecule are shown in Fig. 1. In the ^{1}H–^{1}H COSY spectrum of compound **2** (solvent $CDCl_3$), spin-spin correlations are observed through three bonds of protons of neighboring methylene-methylene morpholine and methine-methine aromatic groups $H^{3.5}$–$H^{2.6}$ (3.05, 3.72 and 3.72, 3.05), H^{11}–H^{12} (7.30, 7.46 and 7.46, 7.30), H^{11}–H^{10} (7.31, 7.77 and 7.77, 7.31) and H^{12}–H^{13} (7.46, 7.85 and 7.85, 7.46) ppm. Heteronuclear interactions of protons with carbon atoms through one bond were established by ^{1}H–^{13}C HMQC spectroscopy (solvent $CDCl_3$) for the following pairs present in the compound: $H^{3.5}$–$C^{3.5}$ (3.03, 52.50), $H^{2.6}$–$C^{2.6}$ (3.71, 66.36), H^{11}–C^{11} (7.30, 128.46), H^{12}–C^{12} (4.46, 132.56), H^{10}–C^{10} (7.76, 131.27), H^{13}–C^{13} (7.85, 126.53), and H^{8}–C^{8} (8.29, 135.30) ppm.

Table 1. ^{1}H and ^{13}C NMR chemical shifts (DMSO-d_6) for compound **2** and β-CD in a free state (δ_0) and in the inclusion complex **2**⊂β-CD (1:1) (δ)

Atom number	Group	δ_0, ppm		δ, ppm		Δδ = δ−δ_0	
		^{1}H	^{13}C	^{1}H	^{13}C	^{1}H	^{13}C
				2			
2ax,6ax	-CH_2-	3.72 d, 3J 3.4 Hz	66.16	3.71 s	66.11	-0.01	-0.05
2eq,6eq		3.72 d, 3J 3.4 Hz	–	3.71 s	–	-0.01	–
3ax,5ax	-CH_2-	3.05 d, 3J 3.4 Hz	51.93	3.04 s	51.91	-0.01	-0.02
3eq,5eq		3.05 d, 3J 3.4 Hz	-	3.04 s	–	-0.01	–
8	=CH-	8.31-8.32 m	136.72	8.30 s	136.64	-0.02	-0.08
9	>C=	–-	134.70	–	134.73	–	0.03
10	=CH-	7.77–7.80 m	130.78	7.74–7.78 m	130.75	-0.02	-0.03
11	=CH-	7.29–7.34 m	128.10	7.29–7.33 m	128.17	0	0.07
12	=CH-	7.44–7.49 m	132.13	7.48–7.59 m	132.11	0.06	-0.02
13	=CH-	7.85–7.88 m	126.22	7.82–7.86 m	126.23	-0.02	0.01
14	>C=	–	132.13	–	132.11	–	-0.02
15	>C=O	–	168.99	–	168.91	–	-0.08
17	-OH	–	–	–	–-	–	–
				β-CD			
1	CH	4.77 s	102.87	4.79 s	102.45	0.02	-0.42
2	CH	3.24 m	72.87	3.26 m	72.90	0.02	0.03
3	CH	3.60 m	73.64	3.59 m	73.57	-0.01	-0.07
4	CH	3.28 m	81.98	3.30 m	82.04	0.02	0.06
5	CH	3.49 m	72.50	3.51 m	72.55	0.02	0.05
6	CH_2	3.60 m	60.42	3.59 m	60.44	-0.01	0.02

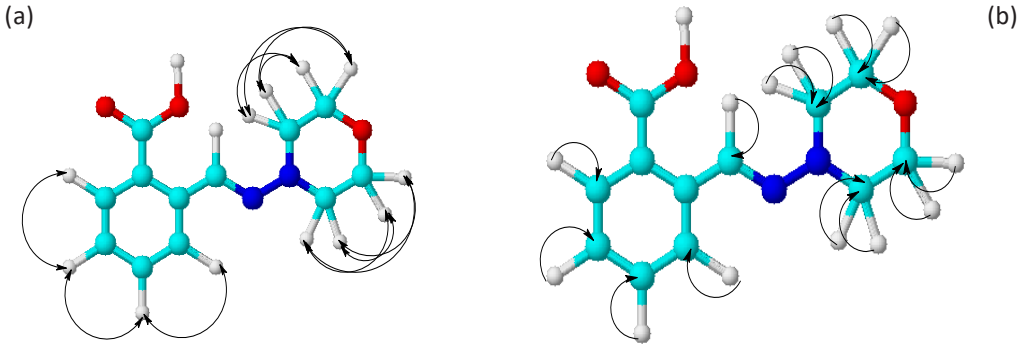

Fig. 1. Scheme of COSY (^{1}H-^{1}H) (a) and HMQC (^{1}H-^{13}C) (b) correlations in molecule **2**.

In the protons of the β-CD molecule, almost no change in chemical shifts is observed. In the guest molecule, few changes in the proton spectra are significant (Δδ = -0.02…0.06) ppm). This shows that the complexation of compound **2** with β-CD is accompanied by not very strong intermolecular interactions. Indeed, during the supramolecular self-assembly of molecule **2** with cyclodextrin macrocycles, just the aromatic proton H-12 undergoes significant change in chemical shift (Δδ = 0.06 ppm). As for the ^{13}C signals of the guest, the azomethine C-8 and carboxylic C-13 are shielded (Δδ = -0.08), while the aromatic C-11 in *para*-position to carboxyl is deshielded (Δδ = 0.07) on the inclusion in the host cavity. Comparison of the integral intensities of the protons of β-CD and compound **2** in the supramolecular complex showed that it coincides with the initial composition of the mixture, and there is one molecule of β-CD per guest molecule **2**.

NMR spectrum ^{1}H of the inclusion complex **3**⊂β-CD in DMSO-d_6 is characterized by the presence of a three-proton singlet at 2.10 ppm assigned to H-20,20,20 of the aceto group (Table 2). Protons H-3ax,5ax and H-3eq,5eq of the morpholine moiety appeared as two-proton multiplets at 3.18–3.23 and 3.29–3.35 ppm, respectively. The remaining morpholine protons H-2ax,6xa,2eq,6eq are observed as a four-proton multiplet at 3.58–3.62 ppm. The tertiary hydrogen atom H-8 (Scheme 1) gave a one-proton singlet at 7.01 ppm. Aromatic protons appeared as multiplets at 7.50–7.51 (H-13), 7.55–7.58 (H-11), 7.62–7.64 (H-12), and 7.65–7.67 (H-10) ppm.

In the ^{13}C NMR spectrum of the **3**⊂β-CD inclusion complex (solvent DMSO-d_6), the signals of the morpholine carbon atoms appeared at 52.43 (C-3,5) and 67.13 (C-2,6) ppm. The resonance of carbon atoms of the aceto group was observed at 21.34 (C-20) and 170.95 (C-17) ppm. The signal of the cyclic tertiary carbon atom C-8 appeared at 81.22 ppm. The aromatic carbon atoms gave signals at 123.26 (C-12), 124.49 (C-13), 130.92 (C-11), 131.31 (C-14), 133.57 (C-10), and 140.26 (C-9) ppm. In the low-field region at 166.18 ppm, a signal of the hydrazide atom C-15 was noted. The structure of the inclusion complex **3**⊂β-CD was also confirmed by two-dimensional NMR spectroscopy COSY (^{1}H–^{1}H), HMQC (^{1}H–^{13}C) and HMBC (^{1}H–^{13}C), which made it possible to determine spin-spin interactions of homo- and heteronuclear nature. Some of the observed correlations in the molecule are shown in Fig. 2. In the ^{1}H–^{1}H COSY spectrum of the compound (solvent DMSO-d_6), spin-spin correlations are observed through three bonds for protons of neighboring methylene-methylene morpholine and methine-methine aromatic groups $H^{3ax,5ax}$–$H^{3eq,5eq}$ (3.20, 3.31 and 3.31, 3.20), $H^{3ax,5ax}$–$H^{2ax,6ax}$ (3.20, 3.59 and 3.59, 3.20), $H^{3eq,5eq}$–$H^{2eq,6eq}$ (3.30, 3.60 and 3.60, 3.30), H^{13}–H^{12} (7.49, 7.62 and 7.62, 7.49), and H^{11}–H^{10} (7.57, 7.66 and 7.66, 7.57) ppm.

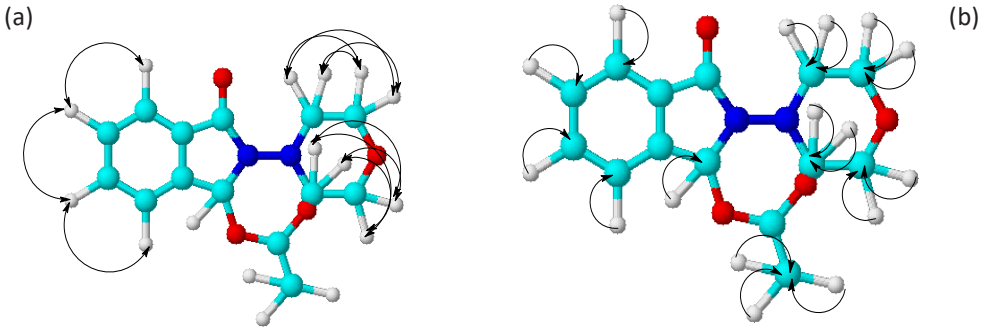

Fig. 2. Scheme of COSY (^{1}H–^{1}H) (a) and HMQC (^{1}H–^{13}C) (b) correlations in molecule **3**.

Table 2. ^{1}H and ^{13}C NMR chemical shifts (DMSO-d_6) for compound **3** and β-CD in a free state (δ_0) and in the inclusion complex **3**⊂β-CD (1:1) (δ)

Atom number	Group	δ_0, ppm		δ, ppm		Δδ = δ − δ_0	
		^{1}H	^{13}C	^{1}H	^{13}C	^{1}H	^{13}C
				3			
2ax,6ax	-CH_2-	3.58–3.62 m	67.13	3.56 s	67.04	-0.04	-0.09
2eq,6eq		3.58–3.62 m	–	3.56 s	–	-0.04	–
3ax,5ax	-CH_2-	3.18–3.23 m	52.43	3.25 s	52.53	0.05	0.10
3eq,5eq		3.29–3.35 m	–	3.31 s	–	-0.01	–
8	>CH-	7.01 s	81.22	6.69 s	81.06	-0.02	-0.16
9	>C=	–	140.26	–	143.98	–	3.72
10	=CH-	7.65–7.67 m	133.57	7.57 s	132.99	-0.09	-0.58
11	=CH-	7.55–7.58 m	130.92	7.48 s	130.02	-0.09	-0.90
12	=CH-	7.62–7.64 m	123.26	7.57 s	122.65	-0.06	-0.61
13	=CH-	7.50–7.51 m	124.49	7.48 s	124.03	-0.02	-0.46
14	>C=	–	131.31	–	131.25	–	-0.06
15	>C=O	–	166.18	–	165.69	–	-0.49
17	>C=O	–	170.95	–	–	–	–
20	-CH_3	2.10 s	21.34	0.98 s	26.03	-1.12	4.69
				β-CD			
1	CH	4.77 s	102.87	4.77 s	102.41	0	-0.46
2	CH	3.24 m	72.87	3.25 m	72.86	0.01	-0.01
3	CH	3.60 m	73.64	3.56 m	73.52	-0.04	-0.12
4	CH	3.28 m	81.98	3.29 m	81.98	0.01	0
5	CH	3.49 m	72.50	3.44 m	72.50	-0.05	0
6	CH_2	3.60 m	60.42	3.56 m	60.15	-0.04	-0.27

Heteronuclear interactions of protons with carbon atoms through one bond were established by ^{1}H–^{13}C HMQC spectroscopy (solvent DMSO-d_6) for the following pairs present in the compound: H^{20}–C^{20} (2.09, 21.58), $H^{3ax,5ax\text{-}C3,5}$ (3.19, 52.28), $H^{3eq,5eq\text{-}C3,5}$ (3.31, 52.41), $H^{2ax,2eq,6ax,6eq}$–C2,6 (3.58, 67.16), H^{11}–C^{11} (7.56, 130.94), H^{12}-C^{12} (7.65, 13.32), H^{10}-C^{10} (7.63, 133.56), H^{13}–C^{13} (7.50, 124.48) and H^{8}–C^{8} (7.00, 81.47) ppm. Heteronuclear interactions of protons with carbon atoms through two or more bonds were established using ^{1}H-^{13}C HMBC spectroscopy for the following pairs present in the compound: H^{20}–C^{17} (2.09, 171.83), H^{8}–C^{14} (6.99, 131.77), H^{8}–C^{9} (6.99, 140.75), H^{8}–C^{15} (7.00, 166.73), and H^{8}–C^{17} (7.00, 171.35) ppm.

In the ^{1}H NMR spectrum of the β-cyclodextrin molecule, noticeable changes in chemical shifts are observed for the H-3 and H-5 protons (Δδ = -0.05… 0.01 ppm). This shows that the complexation of compound **3** with β-CD is accompanied by significant host-guest interactions. During supramolecular self-assembly of molecule **3** with β-CD macrocycle, aromatic protons H-10 and H-11 undergo interaction. Also, the ^{13}C chemical shifts of the guest are changed significantly (Table 2). Comparison of the integral intensities of the β-CD protons and compound **3** in the supramolecular complex showed that it coincides with the initial composition of the mixture, and there is one β-CD molecule per molecule **3**.

When studying structure of complexes, much attention should be paid to the relationship between structural and thermodynamic characteristics during supramolecular complex formation, allowing one to predict the driving forces of interaction and changes in the system associated with the complexation. Modern methods of molecular modeling were used to assess the role of the structural factor and the principle of geometric complementarity in the processes of complex formation between β-cyclodextrin and the investigated guest molecules.

Molecular modeling of «host-guest» complexes

2-((Morpholinoimino)methyl)benzoic acid **2** and 2-morpholino-3-oxoisoindolin-1-yl acetate **3** are potential bioactive compounds that may benefit from cyclodextrin-based formulations to enhance solubility and bioavailability in aqueous environments [14]. β-CD, a cyclic oligosaccharide with a hydrophobic cavity, is widely used for host-guest complexation to improve drug properties, including stability and targeted delivery [15]. The β-CD structure adopts a truncated cone conformation, where the primary rim is lined with seven primary hydroxyl groups from the C-6 positions of the glucopyranose units, while the wider secondary rim features 14 secondary hydroxyl groups from the C-2 and C-3 positions. In aqueous solution, β-CD favors an "open" conformation with the primary hydroxyl groups directed outside the cavity, which enhances cavity accessibility for guest molecules [16]. Considering the stereochemical features of the studied guests – compound **2** as a more stable *E*-isomer (*E*-**2**) and **3** as a chiral molecule – their interactions with β-CD can demonstrate different affinities for the host, which affects the enantioselectivity of complex formation and the overall stability of the complex. In this section, we consider the results of a study of the complex formation of molecule *E*-**2** and the enantiomers of compound **3** (*R*-**3** and *S*-**3**) with β-CD in aqueous solution using computer modeling. Particular attention is paid to the thermodynamic parameters and structural data to determine the potential applications in pharmaceutical design.

A comprehensive computational workflow was employed to study the host-guest complexes between *E*-**2**, *R*-**3**, *S*-**3** and β-CD (see Materials and Methods for additional details). The computational steps included a conformational search for the guest molecules, docking of the obtained conformations into the host cavity, and re-optimization of the complexes. Final refinements were conducted using the DFT method at the ωB97X-D/6-311G(d,p) level of theory [17] with CPCM solvation, incorporating basis set superposition error (BSSE) corrections via the counterpoise scheme [18]. The β-CD molecule in its "open" conformation, which is more stable in aqueous solution [16], was used in our molecular modeling studies. The resulting thermodynamic parameters for the complexation reactions are presented in Table 3.

The computed Gibbs free energies of complexation (ΔG°_{298}) for the β-CD complexes with *E*-**2**, *R*-**3** and *S*-**3** enantiomers are modestly negative, ranging from −2.54 to −3.45 kcal/mol, indicating spontaneous but relatively weak thermodynamic favorability in aqueous solution under standard conditions. In contrast, the enthalpies (ΔH°_{298}) are strongly exothermic, with values between −21.25 and −21.87 kcal/mol, underscoring the dominant role of favorable intermolecular interactions such as hydrogen bonding, van der Waals forces, and hydrophobic effects in driving inclusion. This disparity highlights a characteristic enthalpy-entropy compensation effect prevalent in host-guest complexes, where substantial enthalpic gains are largely offset by entropic penalties arising from conformational restrictions of the guest and host, as well as solvent reorganization upon complex formation [15].

The negative values of Gibbs free energies confirm thermodynamic stability of the complexes, with *R*-**3** displaying the most favorable binding (Table 3), followed by *E*-**2** and *S*-**3**. The difference of 0.9 kcal/mol between *R*-**3** and *S*-**3** indicates a noticeable enantioselective recognition by β-CD toward the *R*-**3** enantiomer, likely attributable to the chiral asymmetry of the cyclodextrin cavity, which imposes differential steric and electrostatic interactions [19]. The open conformation of β-CD in aqueous solution, characterized by flexible primary and secondary rims [20, 21], may enhance accessibility of the cavity for the guests, promoting deeper inclusion and stronger stabilization.

To evaluate the structural changes of β-CD caused by complexation with *E*-**2**, *R*-**3**, and *S*-**3** molecules, we quantified the geometric distortions in the macrocycle by calculating the average distances of key oxygen atoms to the corresponding centroids and determining the standard deviations of these interatomic distances. The listed characteristics were

Table 3. Complexation energies, enthalpies and Gibbs free energies (kcal/mol) for β-CD with *E*-**2** and enantiomers of compound **3** as guest molecules (ωB97X-D/6-311G(d,p), CPCM(water))

Reaction	ΔE	ΔH°_{298}	ΔG°_{298}
β-CD + *E*-**2** → *E*-**2**⊂β-CD	−24.58	−21.83	−3.11
β-CD + *R*-**3** → *R*-**3**⊂β-CD	−24.44	−21.87	−3.45
β-CD + *S*-**3** → *S*-**3**⊂β-CD	−24.06	−21.25	−2.54

obtained for the structures optimized by the ωB97X-D/6-311G(d,p) method and cover the oxygen atoms of the primary and secondary hydroxyl groups, as well as α-1,4-glycosidic bonds. A separate centroid was used for each subset of oxygen atoms. The results for free β-CD and its complexes with *E*-**2**, *R*-**3**, and *S*-**3** are presented in Table 4.

In free β-CD, the primary rim maintains exceptional geometric regularity (average distance: 6.65 Å; RMS deviation: 0.05 Å), reflecting near-symmetrical OH oxygen positioning. The secondary rim and glycosidic oxygen atoms similarly exhibit low variability. Upon forming complexes with *E*-**2** or **3** enantiomers, substantial distortions emerge. For *E*-**2**⊂β-CD, the primary rim's average distance decreases slightly but its RMS deviation increases dramatically to 0.60 Å, signifying marked irregularity. Concurrently, the secondary rim and glycosidic oxygen distances decrease modestly, while their RMS deviations are significantly elevated relative to the uncomplexed state. Identical trends characterize the *R*-**3** and *S*-**3** complexes (Table 4). These results confirm that complexation triggers both cavity contraction (notably at the secondary rim) and widespread loss of structural symmetry, with the primary and secondary rims showing the greatest sensitivity.

These geometric distortions directly reflect guest positioning and host-guest interactions (Fig. 3). In *E*-**2**⊂β-CD, the morpholine ring occupies the cavity, the carboxylic group is hydrogen-bonded with secondary-rim hydroxyls, and the benzene ring extends beyond the secondary rim – driving its contraction and elevated RMS deviations. For **3** complexes, the hydrophobic 3-oxoisoindoline moiety is buried within the cavity, while morpholinoimino and ester groups project from the primary rim, inducing conformational irregularity and increased RMS values at this rim (Table 4). The analysis of the DFT-optimized geometries confirms no hydrogen-bonding interactions between β-CD and **3** enantiomers (Fig. 3b,c) – unlike the carboxylic acid-mediated H-bonding seen in the *E*-**2**⊂β-CD complex (Fig. 3a). Instead, van der Waals forces exclusively drive complexation for both *R*-**3** and *S*-**3**. All the studied complexes disrupt the secondary rim's homodromic hydrogen-bond network [22], causing the rim contraction and higher distortion. Notably, *S*-**3** exhibits the most pronounced asymmetry (secondary rim RMS: 0.66 Å; glycosidic oxygens: 0.16 Å), confirming non-uniform, enantiomer-dependent distortions. This stereochemical sensitivity in structural perturbations likely underpins the enantioselectivity of the complexation.

Table 4. Average distances (in Å) from the centroids and their RMS deviations for oxygen atoms in the primary rim, secondary rim, and glycosidic linkages of β-CD in its uncomplexed form and in the complexes with *E*-**2**, *R*-**3** and *S*-**3**. The geometries were calculated at the DFT level ωB97X-D/6-311G(d,p) with CPCM solvation (water).

System	Primary rim	Secondary rim	Glycosidic bonds
β-CD	6.65 ± 0.05	6.32 ± 0.27*	5.053 ± 0.004
E-**2**⊂β-CD	6.60 ± 0.60	6.26 ± 0.55	5.00 ± 0.10
R-**3**⊂β-CD	6.73 ± 0.68	6.14 ± 0.56	4.96 ± 0.09
S-**3**⊂β-CD	6.83 ± 0.64	5.99 ± 0.66	4.91 ± 0.16

* The noticeable standard deviation for the secondary β-CD rim arises from the non-equivalence of the hydroxyl groups at positions 2 and 3 of the α-D-glucopyranose units.

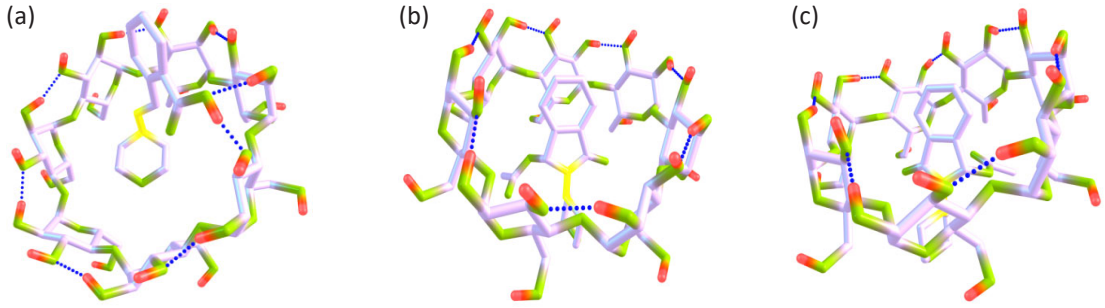

Fig. 3. Optimized structures of the β-CD complexes with *E*-**2** (Panel a), *R*-**3** (Panel b), and *S*-**3** (Panel c). Hydrogen atoms attached to non-carbon atoms are displayed as red tubes, and hydrogen bonds are represented by blue dashed lines.

The NMR spectra provided critical structural hypotheses for the binding modes, identifying key included moieties via diagnostic chemical shift perturbations – such as shielding of azomethine proton H-8 and carbon C-8 in *E*-**2**, and aromatic protons H-10/H-11 alongside tertiary carbon C-8 in compound **3**. These hypotheses were rigorously tested and confirmed through the DFT workflow: semiempirical docking generated multiple poses, from which the lowest-energy configurations were optimized at the ωB97X-D/6-311G(d,p) level, yielding optimized geometries that precisely recapitulated the NMR-inferred inclusions. Overall, the optimized geometries of the inclusion complexes for compounds *E*-**2** and **3** are consistent with the experimental NMR data. Thus, for enantiomers of compound **3**, the 3-oxoisoindoline moiety is included in the β-CD cavity, in agreement with the significant changes in shielding of the protons H-10, H-11 and carbons C-8, C-10, C-11 on complexation (Table 2), alongside deshielding of C-9. For compound *E*-**2**, the azomethine moiety is buried within the host cavity in accordance with a significant shielding effect on C-8 carbon. Also, the COOH group forms a hydrogen bond with the secondary rim of β-CD, which is accompanied with the noticeable changes in chemical shifts of carboxylic carbon C-15 and the C-11 atom in the *para*-position to carboxyl (Table 1).

The stability data (Table 3) confirm enantioselective recognition by β-CD, with *R*-**3** forming a noticeably more stable complex than its *S* counterpart. This preference arises from superior steric compatibility and van der Waals forces between *R*-**3** and the chiral β-CD cavity. Such enantioselectivity aligns with established principles of cyclodextrin host-guest chemistry, where the asymmetric cavity inherently discriminates between enantiomers through differential non-covalent interactions [19].

A comparative analysis of the two guest molecules highlights that *E*-**2** benefits from both strong hydrogen bonding by its carboxylic group to the β-CD secondary rim and hydrophobic burial of the morpholine ring, whereas *R*- and *S*-**3** rely predominantly on van der Waals interactions and steric conformity of the rigid 3-oxoisoindoline core, with the *R* enantiomer exhibiting superior geometric complementarity to the chiral host cavity. This substitution from an open-chain hydrazone carboxylic acid to a cyclic phthalimidine acetate thus shifts the dominant inclusion factors from polar hydrogen bonding to apolar dispersion forces, resulting in a higher stability for *R*-**3** (ΔG°_{298} = −3.45 kcal/mol) over *E*-**2** (−2.54 kcal/mol). These findings elucidate how targeted structural modifications can fine-tune complex stability, offering valuable guidance for designing cyclodextrin-based formulations of bioactive heterocycles.

3. Experimental part

^{1}H and ^{13}C NMR spectra were recorded on a JNM-ECA Jeol 400 spectrometer (frequency 399.78 and 100.53 MHz, respectively) at 20 °C using DMSO-d_6 or $CDCl_3$ solvents. Chemical shifts were measured relative to the signals of residual protons or carbon atoms of the deuterated solvent. Melting points were determined on an SMP10 apparatus. TLC analysis was performed on Silufol UV-254 plates and developed with iodine vapor.

The β-CD molecule was optimized by the DFT method at the ωB97X-D/6-311G(d,p) level of theory using the CPCM solvation model (solvent – water). No symmetry constraints were imposed. After optimization, vibrational analysis was performed. The incorporation of compounds *E*-**2**, *R*-**3**, and *S*-**3** into β-CD was investigated using a stepwise computational approach. First, a conformational study of the guest molecules was performed using the semiempirical GFN2-xTB method [23] in combination with the GOAT algorithm [24] available in the ORCA 6.0.1 package [25]. These calculations allowed us to find 24 conformers for *E*-**2** and 21 conformers for each of the enantiomers of compound **3**. Then, all found conformers were docked into the β-CD cavity in the gas phase using the GFN-FF force field [26] at the evolution stage and the GFN2-xTB method at the optimization stage within the automated docking algorithm implemented in the ORCA program. The obtained docking positions for each host–guest pair were re-optimized by the semi-empirical GFN2-xTB method using the ALPB solvation model [27] (solvent – water) and vibrational frequency calculations (the NumFreq option of ORCA 6.0.1 was used) to determine the Gibbs free energies.

The docking positions with the lowest Gibbs energies for each guest were then optimized by the DFT method at the ωB97X-D/6-311G(d,p) level of theory in the Gaussian 09 program [28] using the CPCM model [29] to account for aqueous solvation. Vibrational analysis allowed us to determine the enthalpies and Gibbs free energies for the host–guest complexes. Selected guest conformations obtained using the GOAT algorithm (see above), chosen based on the lowest Gibbs energies from the GFN2-xTB/ALPB iterative optimizations, were optimized using the same DFT methodology. Basis

set superposition error (BSSE)-corrected enthalpies (ΔH°_{298}) and Gibbs free energies (ΔG°_{298}) of complexation were obtained [18]. Low-frequency vibrational contributions were taken into account using the Grimme interpolation method [30] implemented in the Shermo software [31].

*Inclusion complex of 2-((morpholinoimino)methyl)benzoic acid **2** with β-cyclodextrin (**2**⊂β-CD).* To obtain the inclusion complex of 2-((morpholinoimino)methyl)benzoic acid with β-cyclodextrin, 0.4 g (0.0017 mol) of hydrazone **2** was dissolved in 10 ml of ethyl alcohol and mixed with 1.94 g (0.0017 mol) of β-cyclodextrin in 40 ml of distilled water. The resulting mixture was stirred on a magnetic stirrer at 50–70 °C for 4 h. The mixture was left overnight. The following day, the formed precipitate was filtered off and placed in a vacuum drying oven at 50–55 °C. 1.68 g (72.5%) of the **2**⊂β-CD complex was obtained in the form of a light-yellow powder that decomposed upon melting above 280 °C (Scheme 2).

*The inclusion complex of 2-morpholino-3-oxoisoindolin-1-yl acetate **3** with β-cyclodextrin* (**3**⊂β-CD) was obtained similarly to compound **2**⊂β-CD (Scheme 3) from 0.4 g (0.0014 mol) of 2-morpholino-3-oxoisoindolin-1-yl acetate and 1.64 g (0.0014 mol) of β-cyclodextrin. 1.27 g (66.8%) of the target complex were obtained as a colorless powder (mp 325–330 °C).

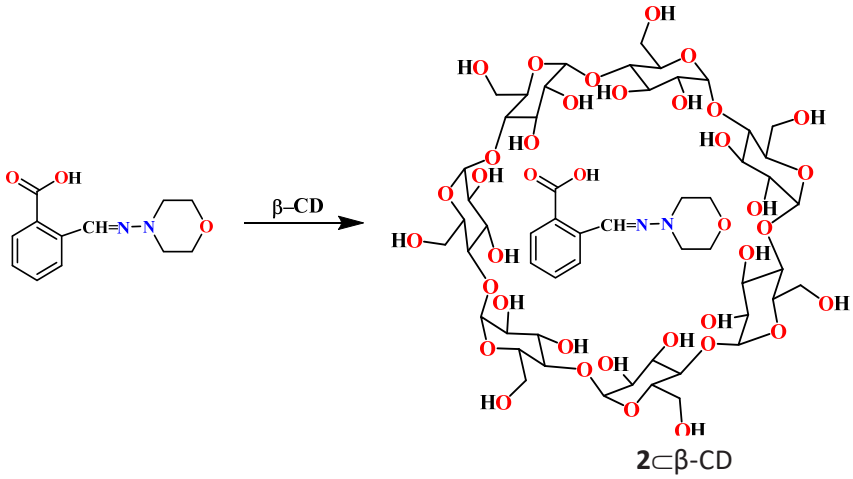

Scheme 2. Synthesis of the inclusion complex with compound **2**.

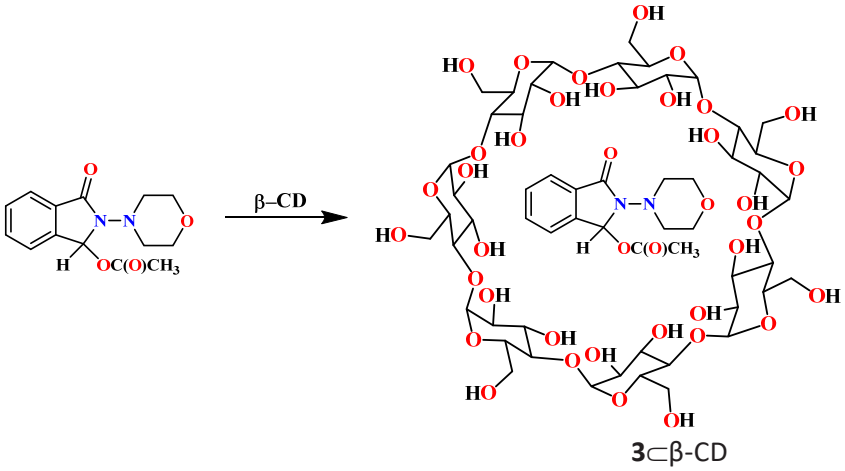

Scheme 3. Synthesis of the inclusion complex with compound **3**.

4. Conclusion

The interaction of β-cyclodextrin with N-aminomorpholine hydrazone and its phthalimidine derivative resulted in the formation of encapsulated forms of their new products. The use of molecular modeling allowed us to evaluate the role of structural factors and the principle of geometric complementarity in the processes of complex formation between the "guest" and "host" molecules. Density functional theory calculations revealed spontaneous complex formations driven by exothermic enthalpies

and hydrophobic/van der Waals interactions with an enantioselective preference for the R-phthalimidine enantiomer. These results demonstrate the potential of the obtained inclusion complexes for enhancing solubility, stability, and bioavailability, as well as their potential for further study as antiviral and antibacterial substrates.

Acknowledgment

This research was funded by the Science Committee of the Ministry of Science and Higher Education of the Republic of Kazakhstan (project No.BR24992921).

The authors express their gratitude to the Ministry of Science and Higher Education of the Russian Federation for financial support (project No. FSWW-2023-0008).

This study was partially carried out using the computing resources of the supercomputer "SKIF Cyberia" at Tomsk State University.

References

[1]. A.E. Khamitova, D.A. Berillo, Overview of Piperidine and Morpholine Derivatives as Promising Sources of Biologically Active Compounds (Review), *Drug development & Registration* 12 (2023) 44–54. DOI: 10.33380/2305-2066-2023-12-2-44-55

[2]. B.G. DelaTorre, F. Albericio, The Pharmaceutical Industry in 2021. An Analysis of FDA Drug Approvals from the Perspective of Molecules, *Molecules* 27 (2022) 1075. DOI: 10.3390/molecules27031075

[3]. A. Kourounakis, D. Xanthopoulos, A. Tzara, Morpholine as a privileged structure: A review on the medicinal chemistry and pharmacological activity of morpholine containing bioactive molecules, *Med. Res. Rev.* 40 (2020) 709–752. DOI: 10.1002/med.21634

[4]. P. Dhiman, M. Bhatia, Pharmaceutical applications of cyclodextrins and their derivatives, *J. Incl. Phenom. Macrocycl. Chem.* 98 (2020) 171–186. DOI: 10.1007/s10847-020-01029-3

[5]. C. Muankaew, T. Loftsson, Cyclodextrin-Based Formulations: A Non-Invasive Platform for Targeted Drug Delivery, *Basic Clin. Pharmacol. Toxicol.* 122 (2018) 46–55. DOI: 10.1111/bcpt.12917

[6]. T.M. Seilkhanov, A.Yu. Ten, Kh.S. Tassibekov, et al., Supramolecular cyclodextrin complexes of biologically active nitrogen heterocycles, *Chem. Bull. Kaz. Nat. Univ.* 3 (2024) 22–33. DOI: 10.15328/cb1379

[7]. Zh.S. Nurmaganbetov, S.D. Fazylov, O.A. Nurkenov, et al., Combined Computational and Experimental Study of Inclusion Complexes of Lupinine and its 1,2,3-triazole Derivative with β-cyclodextrin, *Eurasian Chem.-Technol. J.* 27 (2025) 127–138. DOI: 10.18321/ectj1660

[8]. O.A. Nurkenov, S.D. Fazylov, Z.T. Shulgau, et al., Synthesis, Structure and Antiradical Activity of Functionally Substituted Hydrazides of Isonicotinic Acid, *Eurasian Chem.-Technol. J.* 25 (2023) 121–128. DOI: 10.18321/ectj1502

[9]. O.A. Nurkenov, S.B. Zhautikova, A.I. Khlebnikov, et al., Synthesis and Biological Activity of New Hydrazones Based on N-Aminomorpholine, *Molecules* 29 (2024) 3606. DOI: 10.3390/molecules29153606

[10]. Zh. Xu, Ch. Liu, Sh. Zhao, et al., Molecular Sensors for NMR-Based Detection, *Chem. Rev.* 119 (2019) 195–230. DOI: 10.1021/acs.chemrev.8b00202

[11]. Y. Inoue, NMR Studies of the Structure and Properties of Cyclodextrins and Their Inclusion Complexes, *Annu. Rep. NMR Spectrosc*. 27 (1993) 59–101. DOI: 10.1016/S0066-4103(08)60265-3

[12]. H.J. Schneider, F. Hacket, V. Rudiger, H. Ikeda, NMR Studies of Cyclodextrins and Cyclodextrin Complexes, *Chem. Rev.* 98 (1998) 1755–1785. DOI: 10.1021/cr970019t

[13]. Mansi, P. Khanna, Sh. Yadav, et al., Inclusion complexes of novel formyl chromone Schiff bases with β-Cyclodextrin: Synthesis, characterization, DNA binding studies and in-vitro release study, *Carbohydr. Polym.* 347 (2025) 122667. DOI: 10.1016/j.carbpol.2024.122667

[14]. E.M. Del Valle, Cyclodextrins and their uses: a review, *Process Biochem*. 39 (2004) 1033–1046. DOI: 10.1016/S0032-9592(03)00258-9

[15]. M.V. Rekharsky, Y. Inoue, Complexation Thermodynamics of Cyclodextrins, *Chem. Rev.* 98 (1998) 1875–1918. DOI: 10.1021/cr970015o

[16]. R. Ferrero, S. Pantaleone, M. Delle Piane, et al., On the Interactions of Melatonin/β-Cyclodextrin Inclusion Complex: A Novel Approach Combining Efficient Semiempirical Extended Tight-Binding (xTB) Results with Ab Initio Methods, *Molecules* 26 (2021) 5881. DOI: 10.3390/molecules26195881

[17]. Chai Jeng-Da, M. Head-Gordon, Long-range corrected hybrid density functionals with damped atom–atom dispersion corrections, *Phys. Chem. Chem. Phys.* 10 (2008) 6615–6620. DOI: 10.1039/b810189b

[18]. K.V. Alantev, D.V. Babailova, M.V. Kaplun, et al., Basis Set Superposition Error: Effects of the Boys–Bernardi Correction on the DFT Modeling of Hydrogen Sorption on Low-Dimensional

Carbon Nanomaterials, *Bull. Russ. Acad. Sci. Phys.* 87 (2023) 1667–1674. DOI: 10.3103/S1062873823703860

[19]. A.H. Mazurek, Ł. Szeleszczuk, Current Status of Quantum Chemical Studies of Cyclodextrin Host–Guest Complexes, *Molecules* 27 (2022) 3874. DOI: 10.3390/molecules27123874

[20]. S. Pantaleone, C.I. Gho, R. Ferrero, et al., Exploration of the Conformational Scenario for α-, β-, and γ-Cyclodextrins in Dry and Wet Conditions, from Monomers to Crystal Structures: A Quantum-Mechanical Study, *Int. J. Mol. Sci.* 24 (2023) 16826. DOI: 10.3390/ijms242316826

[21]. W. Khuntawee, M. Karttunend, J. Wong-ekkabut, A molecular dynamics study of conformations of beta-cyclodextrin and its eight derivatives in four different solvents, *Phys. Chem. Chem. Phys.* 19 (2017) 24219. DOI: 10.1039/c7cp04009a

[22]. W. Saenger, T. Steiner, Cyclodextrin Inclusion Complexes: Host–Guest Interactions and Hydrogen-Bonding Networks, *Acta Cryst.* A54 (1998) 798–805. DOI: 10.1107/S0108767398010733

[23]. C. Bannwarth, S. Ehlert, S. Grimme, GFN2-xTB—An Accurate and Broadly Parametrized Self-Consistent Tight-Binding Quantum Chemical Method with Multipole Electrostatics and Density-Dependent Dispersion Contributions, *J. Chem. Theory Comput.* 15 (2019) 1652–1671. DOI: 10.1021/acs.jctc.8b01176

[24]. B. de Souza, GOAT: A Global Optimization Algorithm for Molecules and Atomic Clusters, *Angew. Chem. Int. Ed.* 64 (2025) e202500393. DOI: 10.1002/anie.202500393

[25]. F. Neese, Software Update: The ORCA Program System–Version 6.0, *WIREs Computational Molecular Science* 15 (2025) e70019. DOI: 10.1002/wcms.70019

[26]. S. Spicher, S. Grimme, Efficient Computation of Free Energy Contributions for Association Reactions of Large Molecules, *J. Phys. Chem. Lett.* 11 (2020) 6606–6611. DOI: 10.1021/acs.jpclett.0c01930

[27]. S. Ehlert, M. Stahn, S. Spicher, S. Grimme, Robust and Efficient Implicit Solvation Model for Fast Semiempirical Methods, *J. Chem. Theory Comput.* 17 (2021) 4250–4261. DOI: 10.1021/acs.jctc.1c00471

[28]. M.J. Frisch, G.W. Trucks, H.B. Schlegel, G.E. Scuseria, M.A. Robb, J.R. Cheeseman, G. Scalmani, V. Barone, B. Mennucci, G.A. Petersson, H. Nakatsuji, M. Caricato, X. Li, H.P. Hratchian, A.F. Izmaylov, J. Bloino, G. Zheng, J.L. Sonnenberg, M. Hada, M. Ehara, K. Toyota, R. Fukuda, J. Hasegawa, M. Ishida, T. Nakajima, Y. Honda, O. Kitao, H. Nakai, T. Vreven, J.A. Montgomery, Jr., J.E. Peralta, F. Ogliaro, M. Bearpark, J.J. Heyd, E. Brothers, K.N. Kudin, V.N. Staroverov, R. Kobayashi, J. Normand, K. Raghavachari, A. Rendell, J.C. Burant, S.S. Iyengar, J. Tomasi, M. Cossi, N. Rega, N.J. Millam, M. Klene, J.E. Knox, J.B. Cross, V. Bakken, C. Adamo, J. Jaramillo, R. Gomperts, R.E. Stratmann, O. Yazyev, A.J. Austin, R. Cammi, C. Pomelli, J.W. Ochterski, R.L. Martin, K. Morokuma, V.G. Zakrzewski, G.A. Voth, P. Salvador, J.J. Dannenberg, S. Dapprich, A.D. Daniels, Ö. Farkas, J.B. Foresman, J.V. Ortiz, J. Cioslowski, D.J. Fox, Gaussian 09. Revision C.01. Gaussian, Inc. (2009).

[29]. R.E. Skyner, J.L. McDonagh, C.R. Groom, et al., A review of methods for the calculation of solution free energies and the modelling of systems in solution, *Phys. Chem. Chem. Phys.* 17 (2015) 6174–6191. DOI: 10.1039/c5cp00288e

[30]. S. Grimme, Supramolecular Binding Thermodynamics by Dispersion-Corrected Density Functional Theory, *Chem. - Eur. J.* 18 (2012) 9955–9964. DOI: 10.1002/chem.201200497

[31]. T. Lu, Q. Chen, Shermo: A general code for calculating molecular thermochemistry properties, *Comput. Theor. Chem*. 1200 (2021) 113249. DOI: 10.1016/j.comptc.2021.113249